International Journal of Pharmaceutics 222 (2001) 243–258

international journal of pharmaceutics

www.elsevier.com/locate/ijpharm

Magnetic resonance imaging investigation of the mixing-segregation process in a pharmaceutical blender

N. Sommier [a,c], P. Porion [b], P. Evesque [c], B. Leclerc [a], P. Tchoreloff [a], G. Couarraze [a,*]

[a] *Laboratoire de Physique Pharmaceutique, UMR 8612, Faculté de Pharmacie, Université Paris XI, 5 rue J.B. Clément, 92296 Châtenay-Malabry Cedex, France*

[b] *Centre de Recherche sur la Matière Divisée, UMR 6619, CNRS, 1 bis rue de la Férollerie, 45071 Orléans Cedex 2, France*

[c] *LMSSMat, UMR 8579, Ecole Centrale de Paris, 92295 Châtenay-Malabry Cedex, France*

Received 17 November 2000; received in revised form 26 April 2001; accepted 27 April 2001

Abstract

Magnetic Resonance Imaging (MRI) was used to study the mixing process of binary mixtures of free flowing sugar beads in a Turbula® mixer. In order to make particles MRI-sensitive, some reference beads were doped with an organic oil. Doped and undoped particles were mixed and MRI was used to non-destructively image the particle bed for a given number of mixer rotations (N_R), bead diameter ratio ($R = d_{ref}/d_i$) and rotation speed (V). All the results were quantified on the basis of image analysis to characterise the degree of mixing. Studies showed that for binary mixtures of identical particle size, the mixing was complete after 30 rotations, whereas for beads of different size ($R = 2.8$) a segregated steady state was obtained after nearly 10 rotations. Experiments revealed that segregation appeared as soon as $R = 0.9$. Moreover, the lower the rotation speed, the more segregated the final state was. It appeared that for a filling level greater than 80%, dead regions appeared in the centre of the powder bed. In conclusion, when the particles are non-cohesive, the Turbula® blender perfectly mixes identical beads but segregation occurs for beads of different size after just a few rotations. © 2001 Elsevier Science B.V. All rights reserved.

Keywords: Mixing; Segregation; Magnetic resonance imaging; Turbula®; Segregation index

1. Introduction

Efficient blending and sampling of powders are of critical importance in the manufacture of a wide variety of pharmaceutical solid dosage forms such as tablets and capsules. In systems of free flowing non-identical solid particles both mixing and segregation may occur (Lacey, 1954; Bridgwater, 1976; Fan et al., 1990; Poux et al., 1991). Parameters responsible for segregation are the difference in density, shape, surface properties and size of the mixture constituent particles. Inhomogeneities in the powder blend can result in

* Corresponding author. Tel.: +33-1-46835610; fax: +33-1-46835882.

E-mail address: guy.couarraze@phypha.u-psud.fr (G. Couarraze).

PII: S0378-5173(01)00718-9

increased composition fluctuations through the powder bed, leading to significant variability of the drug content in tablets.

In mixing different kinds of particulate matter, three broad aspects are of great concern. The first is the type of mixer selected and the mode of its operating conditions. The second is the characterisation of the resultant mixture, and the third is the rate and mechanism of the mixing process which depends on the flow characteristics of the particulate matter to be mixed (Fan et al., 1990).

Dry blending processes have been considered in a number of studies (Hogg and Fuerstenau, 1972), but mixtures were often examined using standard invasive sampling methods (Muzzio et al., 1999). Such methods greatly disturb the mixture structure that they intend to measure and are often limited to a few measurements (Muzzio et al., 1997). Consequently, they are poorly suited to perform detailed characterisation of mixtures. In this paper, we describe a non-invasive method for obtaining qualitative and quantitative characterisation of solid–solid mixing experiments. Images achieved by Magnetic Resonance Imaging (MRI) lead to three-dimensional information without any perturbation of the studied system (Nakagawa et al., 1997a). Indeed, MRI can image the entire powder bed without any sampling procedure (Hill et al., 1997a).

Several aspects of the problems associated with mixing have been dealt with in the literature and the types of mixers available have also been discussed (Adams and Baker, 1956; Rose, 1959; Hogg and Fuerstenau, 1972; Metcalfe et al., 1995; Palmieri et al., 1998; Wightman and Muzzio, 1998; Khakhar et al., 1999). In rotating blenders, the flow of particles occurs on the free surface while particles are motionless in the centre of the powder bed. So mixing is due to convective motion of particles in the flowing layer and collisional diffusion. It is now well known that rotating blenders, such as drum and double-cone, are not good mixers (Hill and Kakalios, 1994; Hill et al., 1999; Moakher et al., 2000). Indeed, when particles are identical longitudinal diffusive mixing (parallel to the axis of rotation) is very long (more than 50 rotations) compared to the radial convective mixing (perpendicular to the axis of rotation) which is due to the flow on the free surface (Das Gupta et al., 1991; Moakher et al., 2000). It is even more difficult to obtain an homogeneous mixture when particles are different in size or in density. Indeed, when particles are not similar, one can observe radial segregation in rotating cylinders and double-cone blenders. The consequences of this radial segregation is the accumulation of the larger (or less dense) beads along the inner wall of the container when the smaller (or denser) beads are located in the centre of the powder bed. In addition, after a sufficient time of mixing it is possible to observe an axial segregation of powders when the mixer is cylindrical. In this case, the segregated pattern is composed of bands perpendicular to the axis of rotation which are more or less enriched in each component (Hill et al., 1997b). Nevertheless, all the studied mixers have a one-dimensional motion (because they have a single axis of rotation) and it is of interest to know what is the influence of a three-dimensional motion on the mixing of powders. A three-dimensional movement of a cylindrical container can be achieved in a commercial device which is the Turbula® mixer.

Even if the Turbula® mixer is considered as one of the most frequently used blenders in pharmaceutical development, only a few studies have been conducted about it (Sinay and Tawashi, 1972; Johnson, 1975; Egermann et al., 1985; Van Ooteghem et al., 1989; De Villiers and Van Der Watt, 1990). In most cases, authors had used sampling tools such as thief probes to extract parts of the powder bed (Egermann et al., 1985). Furthermore, they have observed mixing of cohesive powders (Sinay and Tawashi, 1972) within the framework of practical pharmaceutical drug development (Van Ooteghem et al., 1989).

In this work, mixing and segregation of free-flowing particles blended in a Turbula® mixer were investigated experimentally. Different states resulting from the mixing of beads different in size were compared, to the case of particles of identical size which was considered as the reference system. More precisely, images obtained by MRI were then analysed and used to characterise the structure of granular mixtures. Image analysis was used to determine a segregation index on the basis of standard deviation calculations, providing an effective method for performing a quantitative characterisation of the mixture structure (Lacey, 1954; Fan et al., 1970, 1990; Poux et al., 1991). Several previous MRI experiments have been performed using seeds, the relaxation time of which are long enough to provide sufficient MRI signal (Ehrichs et al., 1995a; Hill et al., 1997a; Nakagawa et al., 1997a). In order to introduce only one segregating parameter, namely the difference in size, all the beads of one experiment need to have the same physical properties (true density, shape…). Consequently, binary mixtures were composed of sugar beads of which one of the two species was impregnated by an MRI sensitive solution (Hill et al., 1997a)[BI1]. Indeed, only one of the species was doped in order to see its distribution among the undoped ones. In this work, different parameters concerning both the Turbula® mixer and the sugar beads properties were studied: for a container filled at 2/3 of the height: (i) the mixing and segregation process as a function of the number of rotations; (ii) the effect of the bead diameter ratio; (iii) the Turbula® rotation speed effect. Finally, the filling level of the container was performed on mixtures composed of sugar beads and poppy seeds.

2. Materials and methods

2.1. Mixture preparation

Sugar beads are commonly used as inert cores in capsules and tablets in oral pharmaceutical formulations. They contain not less than 62.5% and not more than 91.5% of sucrose ($C_{12}H_{22}O_{11}$), calculated on the dried basis. They are prepared from crystalline sucrose, which is coated using sugar syrup and a starch dusting powder. Their surfaces are relatively smooth, their shape roughly spherical (see Fig. 1a) and they have a good flowability. From a general point of view, pellets are commonly used in pharmaceutical technology to carry active components and for this reason they can be coated to control the drug release rate, to prevent incompatibility or simply to mask bad flavours (Moreton, 1994; U.S.P. XXIII, 1995).

The main characteristic of the beads used in the present work are resumed in Table 1. In order to use NMR techniques, reference sugar spheres ($d_{ref} = 981$ μm) were doped with the Rhodorsil® 47V20 (Rhône-Poulenc, France) a polydimethylsiloxanic oil ($Si(CH_3)_3$-O-[$Si(CH_3)_2$-O]$_n$-$Si(CH_3)_3$) the kinematics viscosity of which is 20 mm^2 s^{-1} and the molecular mass of which ranges between 2800 and 3200 g mol^{-1}. Sugar beads were doped with a 10% solution of thissilicon oil in methylene chloride in which they are insoluble. Sugar beads were soaked in this solution during 1 h and then dried on a sieve at room temperature (293 K). After evaporation of methylene chloride, sugar beads impregnated

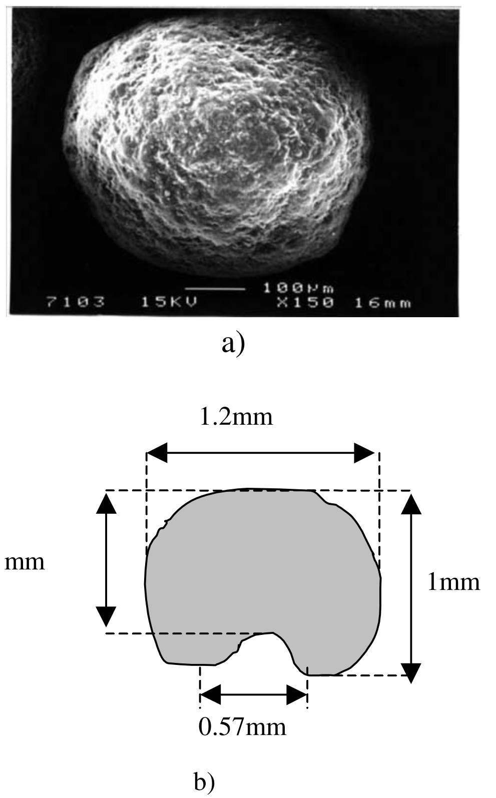

Fig. 1. (a) Sugar beads have a smooth surface and a quite spherical shape implying well-defined sizes. (b) Poppy seeds are MRI-sensitive but they are not spherical as they look like ‘beans’.

Table 1
Main characteristics of sugar beads

d_i	d_{50} (μm)	True density (g cm^{-3})	Specific surface area (m^2 g^{-1})	$R = d_{ref}/d_i$
d_1	352 ± 54	$1.5657 \pm 2 \times 10^{-4}$	$0.168 \pm 2 \times 10^{-3}$	2.8
d_2	469 ± 60	$1.5970 \pm 1 \times 10^{-4}$	$0.200 \pm 2 \times 10^{-3}$	2.1
d_3	592 ± 83	$1.5754 \pm 1 \times 10^{-4}$	$0.306 \pm 4 \times 10^{-3}$	1.6
d_4	684 ± 88	$1.5622 \pm 1 \times 10^{-4}$	$0.254 \pm 2 \times 10^{-3}$	1.4
d_5	839 ± 82	$1.5670 \pm 4 \times 10^{-4}$	$0.243 \pm 6 \times 10^{-3}$	1.2
d_{ref}	981 ± 120	$1.5554 \pm 1 \times 10^{-4}$	$0.244 \pm 4 \times 10^{-3}$	1
d_6	1079 ± 90	$1.5594 \pm 4 \times 10^{-4}$	$0.261 \pm 1 \times 10^{-3}$	0.9
d_7	1548 ± 97	$1.5610 \pm 2 \times 10^{-4}$	$0.286 \pm 1 \times 10^{-3}$	0.6

Diameters are measured by diffraction LASER (Coulter LS230), particle density by Helium pycnometry (Micromeritics, Accupyc 1330) and specific surface area by BET (Coulter SA 3100)

with silicon oil were MRI-sensitive. The flowability of doped and undoped sugar beads has been measured in a Jenike shear cell. Results have showed that the doping process does not introduce any cohesion and both doped and undoped beads are free flowing systems (Sommier, 2000). In addition, the size of the particles measured by laser diffraction (Coulter LS 230) was not affected by the doping process.

For a binary mixture, a bead diameter ratio was defined as $R = d_{ref}/d_i$ where d_i (defined in Table 1) corresponds to the d_{50} of the opposite species.

The Turbula® mixer (Fig. 2) is a commercial device currently used in development laboratories. It is a three-dimensional tumbling mixer and that is why it is of broad interest to study it. The cylindrical mixing chamber is subjected to intensive, periodically pulsating movements, which simulate the pattern of agitation achieved by manual shaking (Johnson, 1975; Spring, 1988; Dirnböck and Stachel, 1997). This extremely complex movement is composed of two rotations of the container around its longitudinal axis and a movement of horizontal translation. Fig. 3 illustrates the motion of the longitudinal axis of the container induced by the mechanism of the Turbula® (Schatz, 1998). In addition of this movement, the container undergoes a rotation around the longitudinal axis of rotation. This three-dimensional motion generates an intricate flow pattern because the free surface changes direction continuously. This is why the flow is called turbulent and the Turbula® considered as a good blender.

A Turbula® mixer of 2 l capacity (W.A. Bachofen, Basle, Switzerland) was used for the mixing investigations. The rotation speed (V) can be set to 22, 32, 48, 68 and 100 rpm.

In order to investigate mixtures in the blending vessel, without any perturbation due to any decanting process of the powder bed, the cylindrical container was 6.5 cm in height and 5.2 cm in

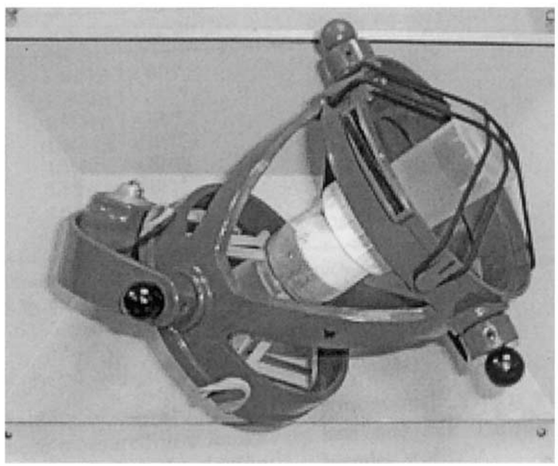

Fig. 2. The Turbula® (W.A. Bachofen, Basle, Switzerland) is one of the most currently used mixers in development laboratories. One can observe the container position in the centre of the device.

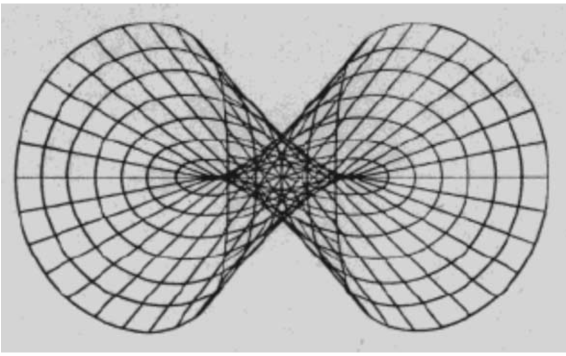

Fig. 3. Schematic motion of the main axis of the cylindrical container in the Turbula®. According to P. Schatz (Schatz, 1998).

diameter. Indeed, these dimensions enable the perfect introduction of the vessel into the MRI probe.

The initial powder bed was always prepared in the same conditions by firstly laying the doped particles in the lower part and then a bed of undoped ones in the upper part. Both powder beds were set in equal volume amounts.

For studies with a variable number of rotations, bead diameter ratio and rotation speed the reference particles were always doped sugar beads and the container was filled to 2/3 of its height.

Concerning, the study of the filling level, the initial state was prepared in the same way except that the doped beads were replaced by poppy seeds (Fig. 1b). Poppy seeds were used instead of doped sugar beads in order to obtain a better signal-to-noise ratio in a shorter time of acquisition. Indeed, it is well-known that seeds have long enough relaxation time to be observed by MRI without any prior preparation (Ehrichs et al., 1995b; Nakagawa et al., 1997b; Hill et al., 1997c).

In all cases the partially filled container was then placed in the centre of the Turbula® to get a symmetric movement (Fig. 2).

2.2. MRI, image analysis and segregation index

The filled cylindrical container, placed in a 56 mm diameter probe head (Bruker mini 036), was imaged at 100 MHz with a Bruker DSX100 spectrometer using a 2.35 T superconducting magnet (CRMD, Orléans, France). Labelling z the cylinder axis, each acquisition of the container gives two series of 16 images, one corresponding to 16 slices parallel to the xy horizontal plane, the other parallel to the vertical zy plane. These experimental conditions allowed to image the entire powder bed present in the container without any sampling. Each image of 64×64 pixels corresponds to a field of 60 mm $\times$ 60 mm which implies that the in-plane resolution was 938 μm and the slice thickness 3.5 mm. In order to obtain a good enough signal-to-noise ratio each acquisition was 20 min long in the case of doped sugar. With poppy seeds as reference beads an acquisition time of 5 min was sufficient. These experiments were performed using selective excitations and the usual two-dimensional Fourier imaging (spin-warp) method (Callaghan, 1991). The two series of 16 slices enable a complete analysis of the distribution of the different grains, since the image intensity shows the MRI active species. Indeed, the image pixel intensity is directly proportional to the concentration of the reference MRI-sensitive beads held in an elementary volume called voxel. Voxel dimensions correspond to the area of a pixel by the slice thicknesss ($0.937^2 \times 3.5$ mm^3). The darker a pixel is, the more numerous the MRI sensitive beads are in the voxel. The partially filled cylinder was rotated in the Turbula® blender, outside the magnet where measurement of the segregation pattern was taken.

The segregation index calculation is frequently used to quantitatively describe powder mixtures. Many definitions, usually based on the standard deviation, have been suggested to express the difference in composition throughout the mixture (Lacey, 1954; Fan et al., 1970, 1990; Poux et al., 1991). Since this index is directly proportional to the standard deviation, the smaller it is, the better the mixing will be. Considering N_v spot samples (i.e. N_v voxels), each containing n particles, the arithmetic mean of pixel intensity value is given by Eq. (1) (Lacey, 1954):

$$\bar{x} = \frac{1}{N_v} \sum_{i=1}^{N_v} x_i, \tag{1}$$

where x_i is the ith value of x which represents a characteristic of the spot sample, such as composition (or pixel intensity in the present case). The sample variance is given by Eq. (2)

$$\sigma^2 = \frac{1}{N_v - 1}\sum_{i=1}^{N_v}(x_i - \bar{x})^2. \tag{2}$$

These experimental values can be compared to σ_0 and σ_R defined as follows for binary mixtures of identical particles. If we consider a binary mixture of similar beads, except in colour (for example doped and undoped beads) where P is the proportion of doped beads and n the total number of beads contained in each voxel. The mean value of number of doped beads is given by:

$$\bar{x} = nP \tag{3}$$

and the variance of a completely segregated system σ_0^2 is given by Eq. (4) (Lacey, 1954; Fan et al., 1970):

$$\sigma_0^2 = n^2 P(1-P). \tag{4}$$

Conversely, in the case of a perfectly random system, the variance σ_R^2 is as calculated in Eq. (5) (Fan et al., 1970):

$$\sigma_R^2 = nP\,(1-P). \tag{5}$$

Consequently, the following relationship can be written,

$$\sigma_R \leq \sigma \leq \sigma_0. \tag{6}$$

In order to quantify segregation by image analysis, we calculated a numerical index S, defined by Eq. (7):

$$S = \frac{\sigma}{\bar{x}} = \frac{\sqrt{1/(N_V - 1)\sum_{i=1}^{N_V}(x_i - \bar{x})^2}}{1/N_V \sum_{i=1}^{N_V} x_i}, \tag{7}$$

where $\bar{x}$ is the mean pixel intensity measured over the totality of the horizontal slices where the powder bed is visible (i.e. from slice 5 to slice 13), σ the standard deviation and $N_v \cong 22\,000$ for this analysis.

Considering that, in the present case $P = 1 - P$, Eq. (6) rewrites in Eq. (8):

$$S_R \leq S \leq S_0, \tag{8}$$

where $S_R = 1/\sqrt{n}$ and $S_0 = 1$. n being about 3.5 beads per voxel, Eq. (8) becomes Eq. (9):

$$0.53 \leq S \leq 1. \tag{9}$$

Because S is defined as a function of σ, it is important to notice that experimentally measured standard deviation will actually be a combination of the true variance resulting from different processes. For this reason σ is classically written as (Poux et al., 1991; Muzzio et al., 1999):

$$\sigma = \sqrt{\sigma_m^2 + \sigma_{se}^2 + \sigma_a^2 + \sigma_{res}^2} \tag{10}$$

where σ_m results from the mixing process, σ_{se} comes from sampling error, σ_a is due to analysis and σ_{res} is the irreducible residual variance induced by the limited number of particles in samples. As the systems studied in this work are not disturbed by sampling practices $\sigma_{se} = 0$ and Eq. (10) rewrites in Eq. (11):

$$\sigma = \sqrt{\sigma_m^2 + \sigma_a^2 + \sigma_{res}^2} \tag{11}$$

This result is of importance since it significantly reduces standard deviation. As a comparison, experiments performed with thief probes can produce up to 100% of maximum sampling errors (Muzzio et al., 1997).

3. Results

3.1. Influence of the number of rotations

Owing to the fact that the movement of the Turbula® is very complex, a well mixed state was expected in each case but it appeared that perfect mixing occurred only for beads of identical size (Fig. 4) for $N_R = 220$ rotations. In order to characterise the mixing/segregation processes, the influence of the number of rotations was investigated. These experiments were carried out on two different mixtures, one containing identical reference particles ($R = d_{ref}/d_{ref} = 1$) and the other containing different-size particles in the ratio $R = d_{ref}/d_1 = 2.8$. Images were taken at different times for a rotation speed of 22 rpm. Resulting images, given in Fig. 5, reveal very complex flow patterns for lower values of N_R which are almost similar for $R=1$ and $R=2.8$. Nevertheless, one can observe that final states reached after $N_R=220$ rotations (Figs. 4 and 5) are extremely different.

The system containing identical particles shows a completely homogeneous composition whereas for particles different in size, one can observe a segregated state. Indeed, in the former case, pixel intensity is quite homogeneous over all the vessel implying a random distribution of doped beads over the powder bed. On the other hand, when $R=2.8$, the heterogeneity of pixel intensity reveals high concentrations of large doped beads along the inner wall of the container and on the free surface. Concerning qualitative observation of the rate processes, segregation is apparently much faster than mixing since for the former case the steady state is almost reached after 10 rotations while for the totally mixed state the steady state is attained after about 30 rotations.

Quantification of these images by segregation-index-calculation confirms these observations as

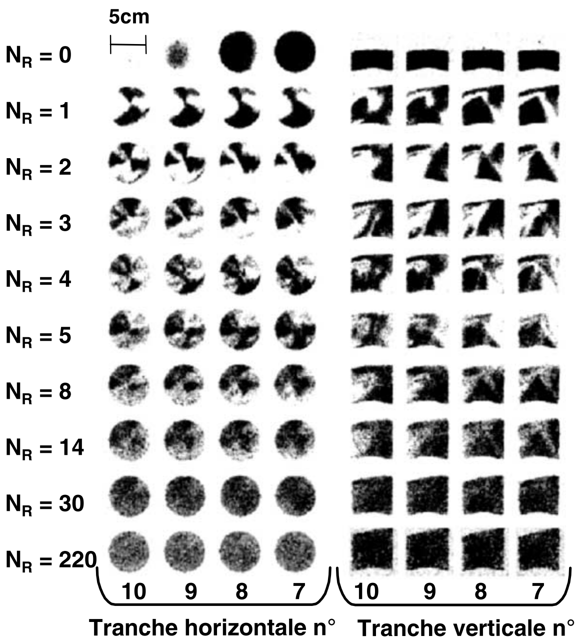

Fig. 4. Influence of the number of rotations when the system is composed of 1 mm doped beads with 1 mm undoped beads (50–50). $R=1$ and $V=22$ rpm. Each line corresponds to the same number of rotations. Images of each column correspond to the same cut at a different rotation.

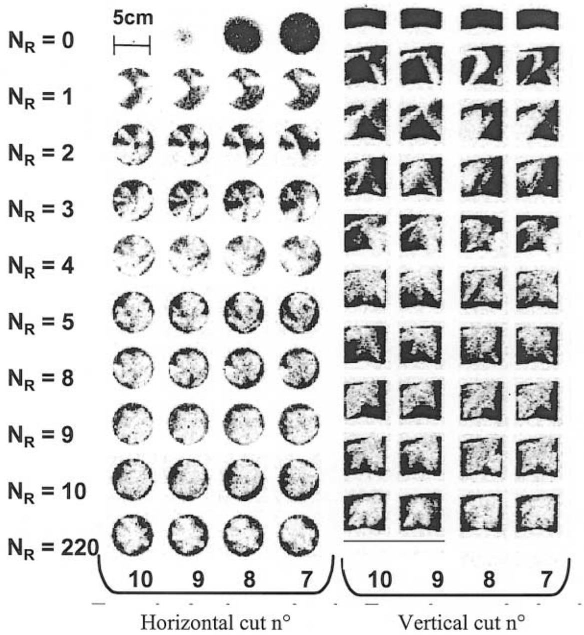

Fig. 5. Influence of the number of rotations when the system is composed of 1 mm doped beads with 0.35 mm undoped beads (50–50). $R=2.8$ and $V=22$ rpm. Each line corresponds to the same number of rotations. Images of each column correspond to the same cut at a different rotation

it can be seen on Fig. 6a which relates S versus number of rotations for the mixing and segregation processes. For $R=1$, one can notice that S decreases from 0.95 to 0.48 with an increasing number of rotations N_R. As S should be included between $S_0=1$ and $S_R=0.53$ (Eq. (9)) the experimental uncertainty is roughly estimated at 10%. This must be due to the irreducible variance induced: (i) by the limited number of voxels (Eq. (11)); and (ii) by the fluctuations of the wall and surface position. One can notice that S variation data can be fitted by mono-exponential curves in the form of Eq. (12):

$$S = S_{i\infty} + A_i e^{-N_R/\tau_i}. \quad (12)$$

This equation leads to two specific parameters which are the characteristic number of rotations τ_i and the asymptotic value $S_{i\infty}$ ($i=$ s, m for segregation and mixing respectively). When $R=1$, it was found that $S_{m\infty}=0.49\pm0.02$, (with a

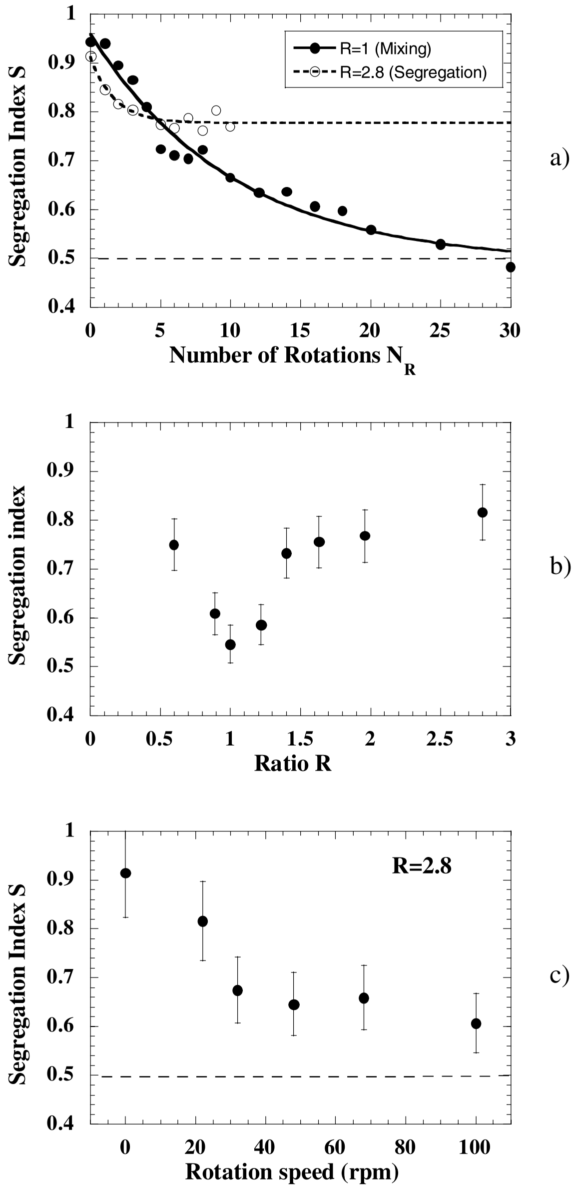

Fig. 6. (a) Segregation index versus number of rotations for $R = 1$ and $R = 2.8$ at 22 rpm. Monoexponential fits highlight that segregation ($\tau_s = 1.4$) is much faster than mixing ($\tau_m = 10.7$). One can define the homogeneous mixture limit as the asymptotic value obtained for $R = 1$. (b) Segregation index S versus bead diameter ratio R after $N_R = 220$ rotations at 22 rpm. (c) Segregation index S versus rotation speed when $N_R = 220$ and $R = 2.8$.

correlation coefficient $C_{cor} = 0.986$ and $A_m = 0.47$). This asymptotic value defines the lower boundary of S (Eq. (9)) and, consequently, will be taken as reference to evaluate the degree of segregation afterwards. Indeed, all following results could be compared to $S_{m\infty}$ in order to give useful information about the quality of mixture. As an example, when $R = 2.8$ the segregation data give an asymptotic value $S_{s\infty} = 0.78 \pm 0.01$ ($A_S = 0.13$, $C_{cor} = 0.922$) which is between 1 and 0.49. This result implies that the final state is less segregated than the initial one but not well mixed since $S_{s\infty} > S_{m\infty}$, which confirms the qualitative observations. Concerning characteristic numbers of rotations, $\tau_s = 1.4 \pm 0.5$ rotations for the segregation process and $\tau_m = 10.7 \pm 1.2$ rotations for the mixing one. As expected from the images, τ_m is larger than τ_s implying that segregation is much faster than mixing. Intermediate characteristic numbers of rotations are expected for beads of diameter ratio between 1 and 2.8.

3.2. Influence of the bead diameter ratio ($N_R = 220$ rotations, $V = 22$ rpm)

In this part, we report results for steady states obtained for given particle size ratios. The bead diameter ratio $R = d_{ref}/d_i$ ranges between 0.6 and 2.8 which implies that undoped beads could be larger or smaller than reference particles. For this reason, first line images of the Fig. 7 are inverted compared to the other ones. Indeed, the doped reference beads are the smaller ones for $R < 1$. It is observed (Fig. 7) that the resulting state varies as a function of R. Indeed, segregation seems to increase when R deviates from one. In order to quantify this phenomenon we related on Fig. 6b, the segregation index S versus R the bead diameter ratio. In absence of finite size, one expects $S(R) \approx S(1/R)$. This is approximately observed in Fig. 6b. As expected qualitatively, the segregation index lower value $S_{min} = 0.54$ is obtained for $R = 1$ and then S increases with increasing or decreasing R. One can observe that the minimal value of S is slightly different than S_∞ defined in the previous part. It is due to the fact that the minimum value of S is different from the asymptotic

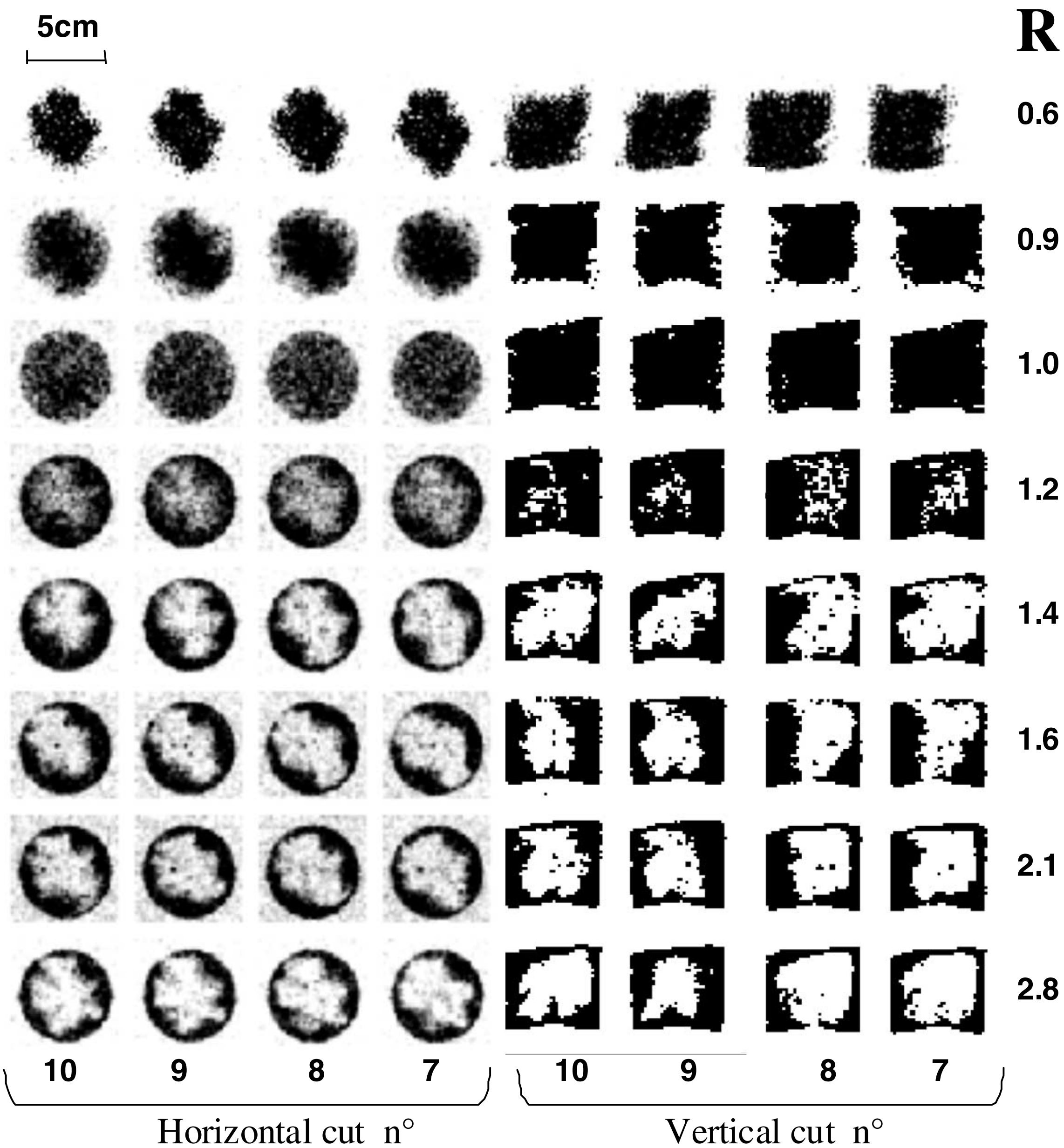

Fig. 7. Influence of the bead diameter ratio after $N_R = 220$ rotations at 22 rpm. Each line corresponds to the same bead diameter ratio and images of each column corresponds to the same cut for a different V.

value obtained from the exponential fit S versus the number of rotations.

Nevertheless, the most important point is that segregation occurs when $R = 0.9$ i.e. for beads almost identical in size.

3.3. Influence of the rotation speed ($R = 2.8$, $N_R = 220$ rotations)

One can observe on Fig. 8 that the segregation pattern of steady states decreases with speed increases. A representation of the segregation index versus rotation speed is given on Fig. 6c which confirms previous qualitative observations in that the segregation index decreases when the rotation speed increases.

Nevertheless, S does not reach $S_{m\infty} = 0.49$ the value obtained for a perfect mixture, this difference shows that, even for the highest speeds, systems remained segregated when $R = 2.8$.

We can also observe that S seems to reach a stationary value when V becomes greater than 32 rpm.

3.4. Influence of filling level

Influence of the filling level was performed on binary mixtures composed of 0.35mm sugar beads and poppy seeds mixed for $N_R = 220$ rotations at $V = 22$ rpm. Poppy seeds were used instead of doped sugar beads in order to obtain a better signal-to-noise ratio. Nevertheless, poppy seeds are not spherical and they look like beans Fig. 1b. Their ratio aspect is 1.2 mm by 1 mm leading to a d_{50} equal to 1.1 mm (Coulter LS 230). Because of difference in size, shape,

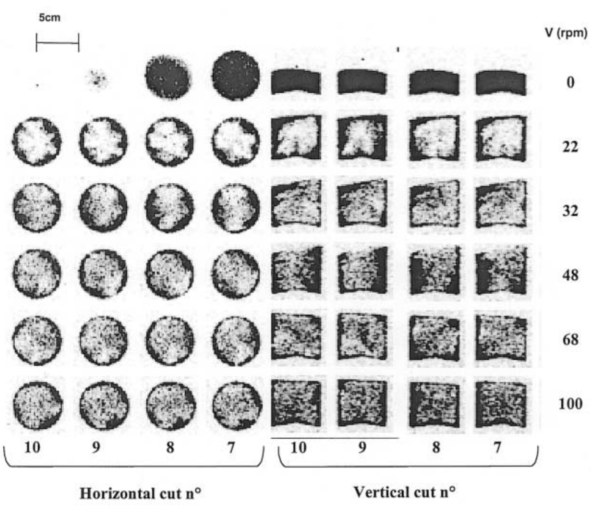

Fig. 8. Influence of the rotation speed when $R = 2.8$ and $N_R = 220$ rotations. Systems are composed of 1 mm doped sugar beads with 0.35 mm undoped ones. Each line corresponds to the same rotation speed V and images of each correspond to the same cut for a different V.

density, and surface properties such systems tend to segregate even more than binary mixtures of sugar beads in which only diameter ratio size had played a part.

When the filling level is lower than 80% of the container volume, the same figures of segregation as described for mixtures of sugar beads are observed (Fig. 9a). Indeed, poppy seeds which are larger than sugar beads, are localised along the inner wall of the container. Nevertheless, it can be noticed that this phenomenon is accentuated because of the additional difference in true density, shape and surface properties. Furthermore, when the filling level of the container exceeds 80%, images reveal that a dead region appears in the centre of the powder bed in addition to the previously studied segregation phenomenon. Bearing in mind that poppy seeds are initially placed in the lower part and sugar beads in the upper part of the container, it is apparent from Fig. 9a that a dead region appears. Indeed, a dark disk observed in the centre of the lower part of the powder bed corresponds to unmoved poppy seeds. In the upper part no disk appears because in this case the unmoved sugar beads are not MRI sensitive and consequently they are invisible. In Fig. 9b, images of a 90% filled container with doped and undoped similar beads confirm that this phenomenon is due to unmoved powder layers in the centre of the Turbula® and do not result from any segregation process. Indeed, perfect mixing is obtained in the outer part of the powder bed.

4. Discussion

4.1. Steady states

In all experiments we obtained perfect mixtures only for identical particles. When the bead diameter ratio is different from one, segregation occurs. Large particles accumulate along the inner part of the container while small particles are located in the inner part of the container.

When $R = 1$ the system is composed of 50% of doped beads and 50% of undoped ones. Be-

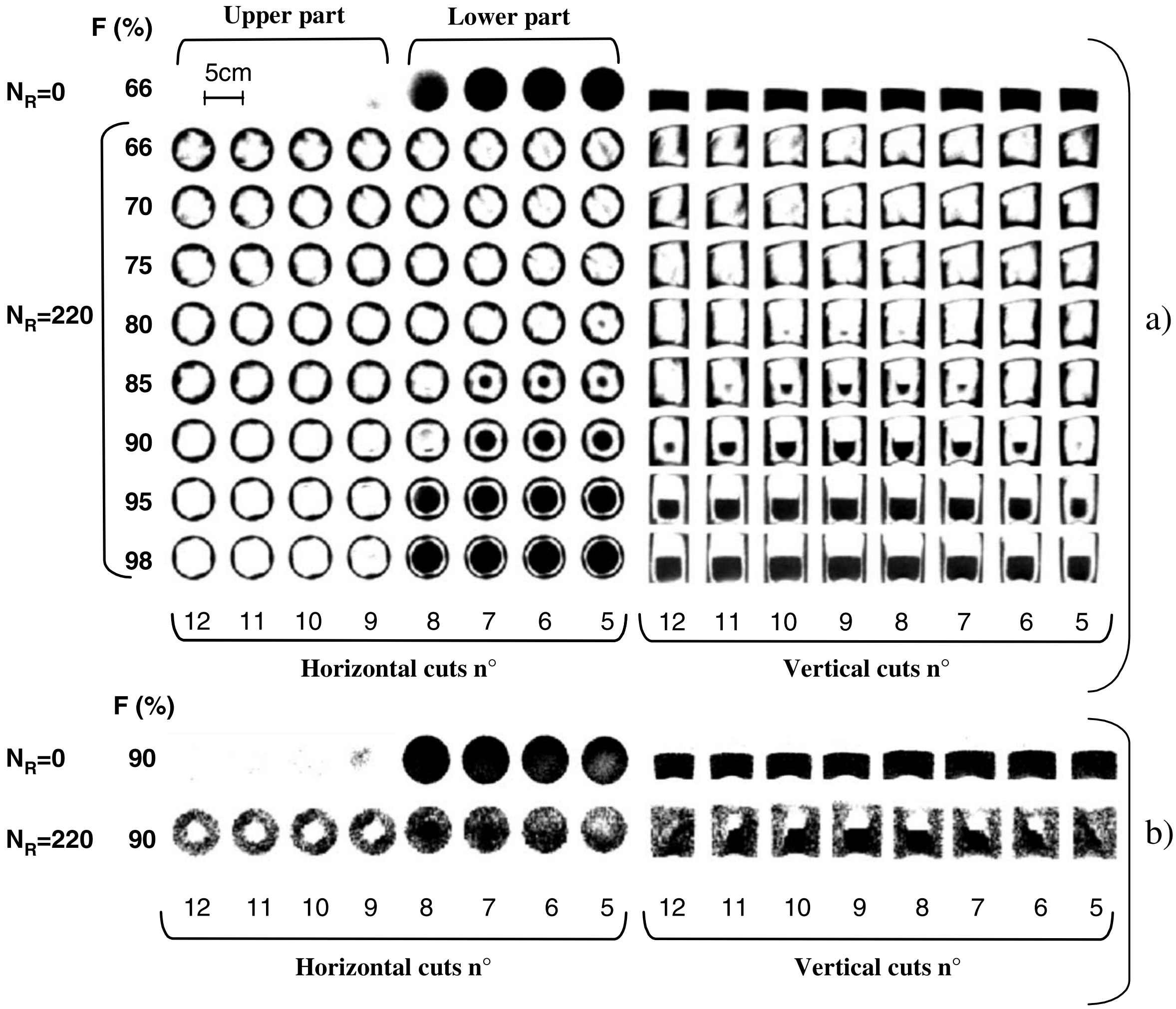

Fig. 9. Influence of the filling level. Each line corresponds to the same filling ratio (F) and images of each column corresponds to the same cut for a different F: (a) poppy seeds with 0.35 mm sugar beads in equal volume proportion; (b) 1 mm doped beads with 1 mm undoped ones.

cause perfect mixing is observed in this case, we can conclude that the doping process has no influence on the flowability. Consequently, segregation observed when $R \neq 1$ is only due to the difference in size. Such a segregation process can be compared to the radial separation of beads occurring in rotating disks were large beads are attracted in the outer part of the powder bed (Muzzio et al., 1997): the segregation process can be explained in terms of percolation in the shear layer during the surface flow. This phenomenon driven by gravity, can be explained by the 'random fluctuating sieve' model of Savage and Lun (Savage and Lun, 1988): the flow takes place in layers which are in motion relative to one another. As a result of overriding and the continual rearrangement of particles within a layer, the contact force network and the void spaces are undergoing continual random changes. If a void space is large enough, then a particle from the layer above can fall into it. This phenomenon is obviously more pronounced when the bead diameter ratio is large because small particles can fall into void spaces more easily. As a consequence of percolation, fine particles in the surface flow enter the powder bed faster than the large ones which can roll farther and reach the wall container (Khakhar et al., 1999).

Nevertheless, even if the segregation pattern in the Turbula® is comparable to radial segregation in rotating drums, there is a non-negligible difference. Indeed, after a sufficient time, it is possible to observe axial segregation in bands in the rotating drum: it is not the case in the Turbula® mixer because of its three-dimensional motion.

4.2. Influence of the number of rotations

We observed on images that the segregation process is faster than the mixing process. This has been confirmed by calculating the segregation index. For $R = 2.8$ and $R = 1$ data have been fitted with an exponential curve from which characteristic numbers of rotations have been deduced.

The characteristic number of rotations for mixing, $\tau_m \approx 10$ rotations, is longer than the characteristic number of rotations of segregation ($\tau_s \approx 1.4$ rotations). For $N = 1$ and 2 we observed on images that the figure is similar in both cases implying that convective motion is not influenced by the bead diameter ratio. This implies that segregation induced by percolation is more efficient than diffusion induced by collisions.

In addition τ_s and τ_m can be compared to the characteristic times of rotation in rotating drum and double-cone blenders in radial planes. As a difference with traditional rotating blenders, there is no problem of long diffusive axial mixing because of the three-dimensional motion of the Turbula® mixer.

4.3. Influence of bead diameter ratio

We observed that segregation increases when increasing bead diameter ratio.

These results are not so surprising since it is well-known that the segregation process is more pronounced if the particle size ratio deviates from $R = 1$ (Williams, 1976). As a comparison, the experimental results from a two-dimensional rotating model indicate that segregation is observed for an arbitrary size ratio (Campbell and Bauer, 1966). In the same way, a numerical approach of the three-dimensional rotating drum operating in the continuous flow regime demonstrated that radial segregation depends linearly on the size ratio and that appears as soon as $R \neq 1$ (Dury and Ristow, 1999). The authors observed that for $R = 2$ the behaviour seems to deviate from the linear curve. These results could be compared to the one of Fig. 6b presenting different behaviour occurring around $R = 1.5$. This could be explained by the fact that for $R \in [1, 1.5]$ collisional diffusion is dominant, whereas for $R > 1.5$, small particles are able to propagate by percolation through the larger beads in the shear layer. This last phenomenon is more pronounced when the difference in size increases. When the size difference is significant, it is easier for a small particle to fall into the voids of the larger particles.

4.4. Influence of rotation speed

We observe that segregation decreases when increasing rotation speed. This phenomenon is explained by the fact that an increase of the speed reduces the relative importance of the gravity (g), compared to the relative vessel acceleration. Labelling the characteristic size of the box L_b ($L_b = 0.05$ m) and the characteristic length of the Turbula® L_T ($L_T = 0.2$ m), this acceleration can be described by introducing two Froude numbers: the first one $Fr_1 = V^2 L_b/g$ takes into account the cell rotation; it ranges from 0.027 to 0.56 in the present work; and the second one, $Fr_2 = V^2 L_T/g$, takes into account the vibration amplitude of the box; it ranges from 0.108 to 2.336 in the present case; this last Froude number becomes quite important at high rotation speed. Consequently, for the higher rotation speeds, the inertia effects are not negligible which then reduces the segregation driven by gravity (percolation). Conversely, for lower rotation speeds, segregation by percolation in the shear layer is predominant.

This could explain why S reaches an asymptotic value when $V = 32$ rpm. This value of V corresponds to $Fr_2 = 1$ that is to say when inertial effects become non-negligible in comparison with gravitational force.

4.5. Influence of the filling level

We observed that a dead region appears in the centre part of the powder when the filling level is greater than 80%. This separation of components is not due to the percolation process because when particles are identical a dead zone appears in the centre part while the powder bed is well mixed in the outer part. This result expresses that the flowing layer responsible for the motion of particles cannot penetrate the centre of the powder bed.

This phenomenon has been observed for tumbling mixers such as rotating disk or double-cone models (Hogg and Fuerstenau, 1972; Metcalfe et al., 1995; Chester et al., 1999). In the case of rotating disk mixers, Metcalfe et al. described a dead region, for slow vessel rotation speed, as a problem of avalanche mixing which can be divided into two distinct parts: transport of wedge and transport between wedges (Metcalfe et al., 1995). They have demonstrated that in a partially filled disk, dead regions appear when the filling level is greater than 50%. However, the process is quite different in the present case were the rotation speed is much higher. In the case of continuous cascading flow obtained at higher speeds, Chester et al. (1999) observed that cascading leads to the formation of smaller cores than those predicted by the wedge model as the unmoved volume below the cascade does not strictly rotate as a solid body. In the present work, it is difficult to apply the wedge model because of the complexity of the Turbula® mixer motion. Nevertheless, one can suppose that the process is similar to the one observed in a double-cone blender even if dead regions in this case appear when the filling level is greater than 50% instead of 80% in our situation. This discrepancy can be explained by the difference in container shape and also the 3-dimensional movement of the Turbula® which is very complex.

The dead region volume increases with the filling level. We can suppose that this is because the length of the free flowing surface reduces with the filling level.

5. Conclusion

MRI is a non-invasive technique, free of sampling procedures, which generally greatly disturb the particle assembly. This method can investigate powder beds and it has been demonstrated that it was as efficient as X-Rays for example (Baxter et al., 1989; Chester et al., 1999). This powerful method can be employed to characterise the mixing of a wide range of systems (particles different in shape, density, etc.). It can be successfully applied to systems where particles lend themselves to a doping process or if their intrinsic NMR relaxation time is long enough, as in the case of poppy seeds, to allow magnetic resonance.

Concerning the blending of free-flowing particles in a Turbula® mixer, some rules arise from these experiments. For a filling volume of the container of less than 80%, particles to be mixed have to be similar in size in order to achieve good mixing. Segregation otherwise occurs as soon as $(d_{max} - d_{min})/d_{max}$ is greater than 10%. In addition, long mixing times which are currently carried out in commercial applications in order to improve mixing quality are irrelevant. Indeed, it was demonstrated in this work that steady states are achieved only after a few number of rotations. The mixing time of identical beads is comparable to the one of the radial mixing time in rotating cylinders and double-cone blenders. Long axial mixing observed in these blenders is not observed in the Turbula® because of its three-dimensional motion (Das Gupta et al., 1991; Moakher et al., 2000). Consequently, for identical beads the Turbula® mixer is more efficient than mixers which have a single axis of rotation. When particles are different in size, we observed radial segregation as in the case of traditional rotating containers and the characteristic times are also comparable. This segregation has been explained in terms of percolation during the surface flow (Savage and Lun, 1988). Nevertheless, we did not observe axial segregation such as band separation of components occurring in the rotating drum. This is due to the three-dimensional motion of the Turbula®.

We observed that mixing is improved with increasing rotation speed, but a well-known triboelectrification of the powders would then induce supplementary uncontrolled phenomena. Furthermore, high rotation speeds are difficult to achieve with large industrial tumbling blenders because of energetic costs.

When the vessel is filled to more than 80%, a persistent dead region is established in the centre of the powder bed. This indicates that it is futile to try mixing powders above a particular reactor filling limit, and that in industrial applications, blending greater volumes per batch would be counterproductive.

In conclusion, we highlighted that the currently used Turbula® mixer was an efficient separator of almost similar free flowing particles. It would be interesting to study its mixing efficiency with cohesive particles and it is expected in this case that segregation would be avoided because of interparticle adhesion strengths. Nevertheless, this should not have any influence on dead region appearance for containers filled to more than 80%.

Acknowledgements

It is a pleasure to acknowledge F. Agnely and M. Besnard for their help concerning the doping process and characterisation of beads. We would like to thank M.P. Faugère for her technical assistance and L. Pothuaud for numerous discussions concerning image processing development. P. P. cordially thanks Dr P. Levitz and Prof. H. Van Damme (CRMD, Orléans, France) for their encouragements. N. S. especially thanks the research team of the CRMD for allowing MRI experiments and for their hospitality. Sugar beads were supplied by P. Sanial from the NP Pharm company and the Bruker spectrometer and minicomputers used in this study were purchased thanks to grants from CNRS and Région Centre (France).

Appendix A

Nomenclature

d_{ref}	diameter of the reference beads ($d_{ref} = 0.9$ mm)
d_i	undoped sugar bead diameter
F	filling level of the container (%)
Fr	Froude number
N	number of beads per voxel
N_R	number of rotations
N_V	number of voxels
P	doped beads concentration
R	beads diameter ratio ($R = d_{ref}/d_i$)
S	segregation index
$S_{m\infty}$, $S_{s\infty}$	experimental asymptotic value of the segregation index obtained by monoexponetial fits for mixing and segregation
S_0, S_R	theoretical S values for completely segregated system and perfectly mixed system
V	rotation speed of the Turbula® mixer (rpm or rad.s^{-1} for Froude Number calculation)
$\bar{x}$	mean pixel intensity of horizontal slices calculated over the totality of the powder bed
x_i	intensity of the i-th pixel
σ	experimental measured standard deviation
σ_0	theoretical standard deviation for a totally segregated system
σ_R	theoretical random (perfect) mixture standard deviation
σ_m	standard deviation resulting from mixing process
σ_a	standard deviation resulting from analysis
σ_{res}	residual standard deviation induced by the number of particles in a sample
σ_{se}	standard deviation resulting from sampling error
τ_s, τ_m	characteristic number of rotations for segregation and mixing obtained from monoexponential fits

References

U.S. Pharmacopeia XXIII, 1995. U.S. Pharmacopeial convention. Rockville, M.D. pp. 2313.

Adams, J.F.E., Baker, A.G., 1956. An assessment of dry blending equipment. Trans. Inst. Chem. Eng 34, 91–107.

Baxter, G.W., Behringer, R.P., Fagert, T., Johnson, G.A., 1989. Pattern-formation in flowing sand. Phys. Rev. Lett. 62, 2825.

Bridgwater, J., 1976. Fundamental powder mixing mechanisms. Powder Technol. 15, 215–236.

Callaghan, P.T., 1991. Principles of Nuclear Magnetic Resonance Microscopy, Oxford.

Campbell, H., Bauer, W.C., 1966. Cause and cure of demixing in solid–solid mixers. Chem. Eng. 73, 179–185.

Chester, A.W., Kowalski, J.A., Coles, M.E., Muegge, E.L., Muzzio, F.J., Brone, D., 1999. Mixing dynamics in catalyst impregnation in double-cone blenders. Powder Technol. 102, 85–94.

Das Gupta, S., Khakhar, D.V., Bhatia, S.K., 1991. Axial transport of granular solids in horizontal rotating cylinders. Part I: Theory. Powder Technol. 67, 145–151.

De Villiers, M.M., Van Der Watt, J.G., 1990. Dissolution rate a measurement of the deaggregation of Furomesides agglomerates during mixing process. Drug Dev. Ind. Pharm. 16, 1391–1397.

Dirnböck, H., Stachel, H., 1997. The development of the Oloid. J. Geom. Graph. 1, 105–118.

Dury, C.M., Ristow, G.H., 1999. Competition of mixing and segregation in rotating cylinders. Phys. Fluids 11, 1387–1394.

Egermann, H., Kemptner, I., Pichler, E., 1985. Effect of interparticulate interactions on mixing homogeneity. Drug Dev. Ind. Pharm. 11, 663–676.

Ehrichs, E.E., Jaeger, H.M., Karczmar, G.S., Knight, J.B., Kuperman, V.Yu., Nagel, S.R., 1995a. Granular convection observed by magnetic resonance imaging. Science 267, 1632–1634.

Ehrichs, E.E., Jaeger, H.M., Karczmar, G.S., Knight, J.B., Kuperman, V.Yu., Nagel, S.R., 1995b. Granular convection observed by Magnetic Resonance Imaging. Science 267, 1632–1634.

Fan, L.T., Chen, Y.-M., Lai, F.S., 1990. Recent developments in solids mixing. Powder Technol. 61, 255–287.

Fan, L.T., Chen, Y.-M., Watson, C.A., 1970. Solids mixing. Ind. Eng. Chem. 62, 53–69.

Hill, K.M., Caprihan, A., Kakalios, J., 1997b. Axial segragation of granular media rotated in a drum mixer: pattern evolution. Phys. Rev. E 56, 4386–4393.

Hill, K.M., Kakalios, J., 1994. Reversible axial segregation of binary mixtures of granular materials. Phys. Rev. E 49, R3610–R3613.

Hill, K.M., Kakalios, J., Tsuji, Y., Yamane, K., Caprihan, A., 1997a. Dynamic angle of repose as a function of mixture concentration: results from MRI experiments and DEM simulations. Powder and Grains 97, 483–486.

Hill, K.M., Kakalios, J., Tsuji, Y., Yamane, K., Caprihan, A., 1997c. Dynamic angle of repose as a function of mixture concentration: Results from MRI experiments and DEM simulations. Powder and Grains 97, 483–486.

Hill, K.M., Khakhar, D.V., Gilchrist, J.F., McCarthy, J.J., Ottino, J.M., 1999. Segregation-driven organization in chaotic granular flows. Proc. Natl. Acad. Sci. 96, 11 701–11 706.

Hogg, R., Fuerstenau, D.W., 1972. Transverse mixing in rotating cylinders. Powder Technol. 6, 139–148.

Johnson, M.C.R., 1975. The effect of particle size upon mixture homogeneity. Pharm. Acta Helv. 50, 60–63.

Khakhar, D.V., McCarthy, J.J., Gilchrist, J.K., Ottino, J.M., 1999. Chaotic mixing of granular materials in two dimensional tumbling mixers. Am. Inst. Phy. 9, 195–205.

Lacey, P.M.C., 1954. Developments in the theory of particle mixing. J. Appl. Chem 4, 257–287.

Metcalfe, G., Shinbrot, T., McCarthy, J.J., Ottino, J.M., 1995. Avalanche mixing of granular solids. Nature 374, 39–41.

Moakher, M., Shinbrot, T., Muzzio, F.J., 2000. Experimentally validated computations of flow, mixing and segregation of non-cohesive grans in 3D tumbling blenders. Powder Technol. 109, 58–71.

Moreton, R.C., 1994. Handbook of Pharmaceutical Excipients, American Pharmaceutical Association, Washington, p. 510

Muzzio, F.J., Robinson, P., Wightman, C., Brone, D., 1997. Sampling practices in powder blending. Int. J. Pharm. 155, 153–178.

Muzzio, F.J., Roddy, M., Brone, D., Alexander, A.W., Sudah, O., 1999. An improved powder-sampling tool. Pharm. Technol. 23, 92–110.

Nakagawa, M., Altobelli, S.A., Caprihan, A., Fukushima, E., 1997a. NMR measurement and approximate derivation of the velocity depth-profile of granular flow in a rotating, partially filled, horizontal cylinder. Powder and Grains 97, 447–449.

Nakagawa, M., Altobelli, S.A., Caprihan, A., Fukushima, E., 1997b. NMR measurement and approximate derivation of the velocity depth-profile of granular flow in a rotating, partially filled, horizontal cylinder. Powder and Grains 97, 447–449.

Palmieri, G.F., Lovato, D., Marchitto, L., Zanchetta, A., Martelli, S., 1998. Evaluation of the mixing effectiveness of a new powder mixer. Drug Dev. Ind. Pharm. 24, 81–88.

Poux, M., Fayolle, P., Bertrand, J., Bridoux, D., Bousquet, J., 1991. Powder mixing, some practical rules applied to agitated systems. Powder Technol. 68, 213–234.

Rose, H.E., 1959. Suggested equation relating to the mixing of powders and its application to the study of the performance of certain type of machine. Trans. Inst. Chem. Eng 37, 47–64.

Savage, S.B., Lun, C.K.K., 1988. Particle size segregation in inclined chute flow of dry cohesionless granular solids. Journal of Fluid Mechanics 189, 311–335.

Schatz, P., 1998. Research of rhythm and technology, Verlag freis Geistesleben, Stuttgart.

Sinay, Y., Tawashi, R., 1972. Etude de mélanges solides-solides; facteurs dynamiques et géométriques. Pharm. Acta Helv. 47, 265–272.
Sommier, N., 2000. Etude du mélange et de la ségrégation de systèmes granulaires non cohésifs et applications pharmaceutiques. Ph.D Thesis, University Paris XI, France.
Spring, M.S., 1988. Blenders and blending operations. In: Encyclopedia of pharmaceutical technology, Vol. 2; New York, pp. 172–188.
Van Ooteghem,M., Van der Jonckheyd,C., Ludwig,A., De Winter,B., 1989. Les facteurs influençant la transposition d'échelle de mélanges de poudres dans un mélangeur Turbula. 5eme Congrès International de Technologie Pharmaceutique (APGI), 4, 390–391.
Wightman, C., Muzzio, F.J., 1998. Mixing of granular material in a drum mixer undergoing rotational and rocking motions. I. Uniform particles. Powder Technol. 98, 113–124.
Williams, J.C., 1976. Continuous mixing of solids. A review. Powder Technol. 15, 237–243.